

# PARALLEL CONNECTION OF DOUBLY-FED INDUCTION GENERATOR IN WIND GENERATION

Francisco Kleber de A. Lima

Edson H. Watanabe

COPPE/Universidade Federal do Rio de Janeiro

Programa de Engenharia Elétrica

Caixa Postal 68504 – 21945-970 – Rio de Janeiro – RJ – Brasil

kleber@coe.ufrj.br, watanabe@coe.ufrj.br

**Abstract** – This work analyzes the behavior of parallel connected doubly-fed induction generators (DFIG) for wind generation application. Field oriented control based on stator magnetic flux is used to regulate the rotor speed in such a way as to guarantee maximum power point tracking (MPPT). The rotor- and grid-side converters are current regulated voltage source converters (VSC). It is shown that with this control scheme the machine behaves as a current source and that the parallel connection of various generators is not a problem for transients in wind speed. However, transients in the grid-side voltage may lead to some current oscillations. The analysis is validated by simulation studies.

**Keywords** – Doubly fed induction generator, vector control and speed control.

## I. INTRODUCTION

One of the greatest Challenges of the industrial development policies of a nation is to generate means to increase the productivity. However to reach such development, the availability of electric energy is an essential condition.

Nowadays one of the most important environmental concerns of the governors and scientific community is the global warning caused by emission of polluters produced from burning of fossil fuel. They are launched in the atmosphere causing the greenhouse effect which brings several harmful consequences to our planet.

Thus, renewable sources of energy arise as a promising solution to this environmental problem, moreover, they bring many employment opportunity and help the nation's social development.

In the last years we have noticed a significant growth in the energy coming from wind generation, mostly in Europe, India and USA.

In Brazil such growth is noticed but it is still shy. Until 2005 the wind electric energy power was about 28 MW. In the beginning of 2007 it is 237 MW coming from 15 wind farm [1]. Such power is equivalent to 0.23% of the total electric power generation facilities installed in the country, which is close to 100 GW. In Denmark, this percentage is 23%.

Nevertheless, here in Brazil these numbers have a lot of space to grow, with the new incentive policy to programs like PROINFA. Statistics issued by ANEEL (Agência Nacional de Energia Elétrica) state that our approved wind energy power reaches 4.7 GW [2], for installation in near future.

Thus, the study and the conception of accurate mathematical models, which best approach reality of wind generation systems are necessary.

Among many works published in Brazil on this subject, most of them analyze wind generator systems based on synchronous machines, which is connected to the grid through Voltage Source Converter (VSC). This system operates at variable speed. The systems based on squirrel cage induction machine, can be connected straightway to the grid. This uses the concept of fixed speed system. A summary about wind generation system is shown in Fig. 1.

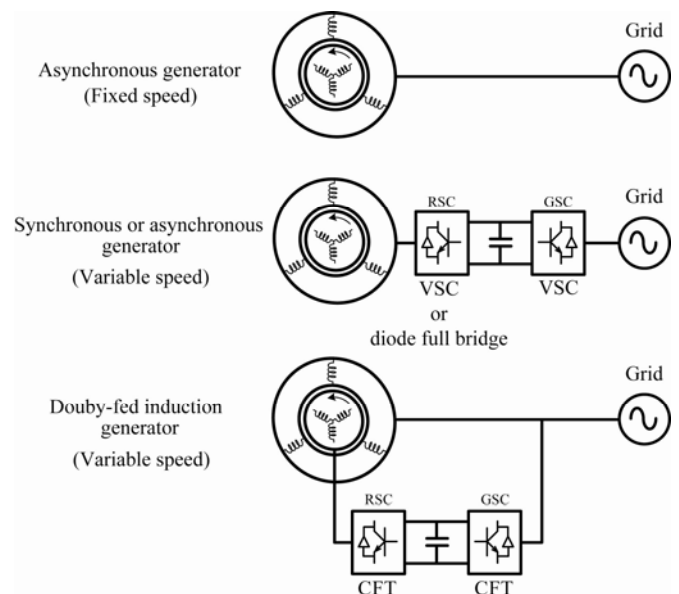


Fig. 1. Wind systems configurations.

In this paper, the development of the model for the doubly-fed induction generator (DFIG) [3]-[9] is presented and it is shown that for parallel operation conditions there are no problems for this systems, when transient occurs at the wind speed. However, transients in the stator voltage may lead to current oscillations. Simulations studies based on PSCAD/EMTDC were developed to validate the analysis.

## II. MATHEMATICAL MODELING OF DFIG

The mathematical model presented here for this machine uses the  $d$ - $q$  synchronous reference frame. Therefore, the following equations can be written for the stator and rotor windings:

$$v_{sd} = R_s i_{sd} + \frac{d\psi_{sd}}{dt} - j\omega_s \psi_{sq}, \quad (1)$$

$$v_{sq} = R_s i_{sq} + \frac{d\psi_{sq}}{dt} + j\omega_s \psi_{sd}, \quad (2)$$

$$v_{rd} = R_r i_{rd} + \frac{d\psi_{rd}}{dt} - j\omega_{sl} \psi_{rq}, \quad (3)$$

$$v_{rq} = R_r i_{rq} + \frac{d\psi_{rq}}{dt} + j\omega_{sl} \psi_{rd}, \quad (4)$$

where:

- $v_{sd,q}$  - Stator voltages in  $d$ - $q$  (synchronous) axes,
- $v_{rd,q}$  - Rotor voltages in  $d$ - $q$  (synchronous) axes,
- $i_{sd,q}$  - Stator currents in  $d$ - $q$  (synchronous) axes,
- $i_{rd,q}$  - Rotor currents in  $d$ - $q$  (synchronous) axes,
- $R_{s,r}$  - Stator and rotor resistances per phase,
- $\omega_{s,sl}$  - Stator flux and slip angular frequency,
- $\psi_{s,dq}$  - Stator flux in  $d$ - $q$  (synchronous) axes,
- $\psi_{r,dq}$  - Rotor flux in  $d$ - $q$  (synchronous) axes.

The  $d$ - $q$  synchronous reference frame equations of the stator flux and rotor may be written as:

$$\psi_{sd} = L_s i_{sd} + L_m i_{rd}, \quad (5)$$

$$\psi_{sq} = L_s i_{sq} + L_m i_{rq}, \quad (6)$$

$$\psi_{rd} = L_r i_{rd} + L_m i_{sd}, \quad (7)$$

$$\psi_{rq} = L_r i_{rq} + L_m i_{sq}, \quad (8)$$

where:

- $\psi_{sd,q}$  - Stator flux in  $d$ - $q$  (synchronous) axes,
- $\psi_{rd,q}$  - Rotor flux in  $d$ - $q$  (synchronous) axes,
- $L_{sd,q}$  - Stator inductance in  $d$ - $q$  (synchronous) axes,
- $L_{rd,q}$  - Rotor inductance in  $d$ - $q$  (synchronous) axes,
- $L_m$  - Magnetizing inductances.

The stator flux vector is used here to orient the  $d$ -axis of the vector control technique [10][11], as shown in Fig. 2.

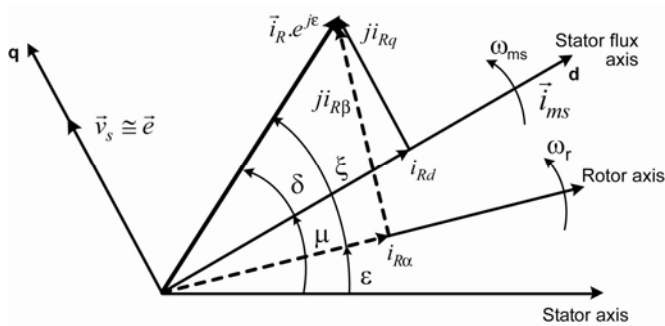


Fig. 2. Angular relationships of current vectors for DFIG.

According to Fig. 2, it follows that  $\psi_{sq} = 0$  and  $v_{sd} \cong 0$ .

Thus, the equations of the electromagnetic torque, active and reactive power, may be written as:

$$T_e = -\frac{3}{2} p \psi_{sd} i_{sq}, \quad (9)$$

$$P_s = \frac{3}{2} v_{sd} i_{sd}, \quad (10)$$

$$Q_s = -v_{sq} i_{sd}, \quad (11)$$

where:

- $T_e$  - Electromagnetic torque,
- $P_s$  - Stator active power,
- $Q_s$  - Stator reactive power,
- $p$  - Numbers of pairs of poles.

The system dynamics, neglecting the friction loss, is given by:

$$J \frac{d\omega_r}{dt} = T_{mec} - T_e, \quad (12)$$

where:

- $T_e$  - Electromagnetic torque,
- $\omega_r$  - Rotor angular speed,
- $T_{mec}$  - Mechanical torque,
- $J$  - Rotor moment of inertia.

## III. CURRENT SOURCE BEHAVIOR OF THE DFIG

Substituting (5) and (6) in (1) and (2), respectively, and performing some mathematical operations the expressions of the  $dq$ -axes stator current components are given by:

$$i_{sd} = \frac{(sL_s + R_s) v_{sd} + \omega_s L_s v_{sq}}{(s^2 L_s^2 + 2sL_s R_s + R_s^2 + \omega_s^2 L_s^2)} - \frac{(s^2 L_s + sR_s + \omega_s^2 L_s) L_m i_{rd} + R_s \omega_s L_m i_{rq}}{(s^2 L_s^2 + 2sL_s R_s + R_s^2 + \omega_s^2 L_s^2)}, \quad (13)$$

$$i_{sq} = \frac{-\omega_s L_s v_{sd} + (sL_s + R_s) v_{sq}}{(s^2 L_s^2 + 2sL_s R_s + R_s^2 + \omega_s^2 L_s^2)} - \frac{R_s \omega_s L_m i_{rd} - (s^2 L_s + sR_s + \omega_s^2 L_s) L_m i_{rq}}{(s^2 L_s^2 + 2sL_s R_s + R_s^2 + \omega_s^2 L_s^2)}. \quad (14)$$

In equations (13) and (14) the stator current in  $dq$ -axes depend on the rotor current in these axes and on the grid voltage. It is possible to simplify these equations, considering that  $v_{sd} \cong 0$  and neglecting the stator resistance. This last

assumption is possible, because in MW-level machines the stator resistance is very low (about 0.01 pu).

When the just described simplification is applied (13) and (14), respectively, become the following:

If  $v_{sq}$  varies then (13) and (14) can be written as:

$$i_{sd} = \frac{1}{L_s} \frac{\omega_s}{(s^2 + \omega_s^2)} v_{sq} - \frac{L_m}{L_s} i_{rd}, \quad (15)$$

$$i_{sq} = \frac{1}{L_s} \frac{s}{(s^2 + \omega_s^2)} v_{sq} - \frac{L_m}{L_s} i_{rq}. \quad (16)$$

However, if  $v_{sq}$  is constant (13) and (14) can be written as:

$$i_{sd} = \frac{1}{L_s \omega_s} v_{sq} - \frac{L_m}{L_s} i_{rd}, \quad (17)$$

$$i_{sq} = -\frac{L_m}{L_s} i_{rq}. \quad (18)$$

In accordance with (17) and (18), the stator currents have the same variations as those of the rotor.

Fig. 3 shows the DFIG in accordance with the equations so far developed equivalent system.

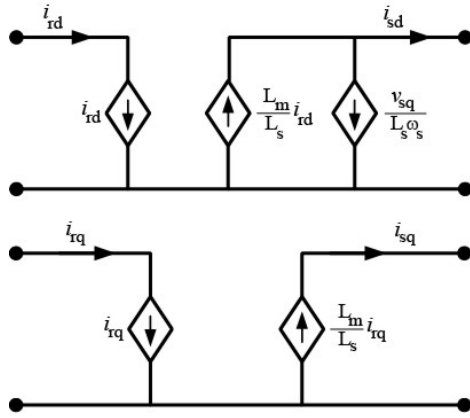


Fig. 3. DFIG model in dq-axes for steady state.

We can conclude through this modeling that, while the grid voltage is constant, wind turbines based on DFIG can be connected in parallel without interference among its controls.

Notice that, when  $v_{sq}$  varies the currents  $i_{sd}$  and  $i_{sq}$  have oscillations as shown through sine and cosine function present in (15) and (16). That is to say there are eigenvalues over the imaginary axis due to making  $R_s$  equal to zero. However, the real values of the stator resistance in spite of being low, they are able to damp oscillations in stator current (poorly damped oscillations). Thus, if  $v_{sq}$  varies, there is no more the current source behavior in this model.

## IV. SIMULATION RESULTS

In this section, simulation results are shown in order to confirm that while the grid voltage is constant, wind turbines based on DFIG can be connected in parallel. The simulation was developed using PSCAD/EMTDC. The simulated system uses field oriented control technique where the stator magnetic flux is used as the reference for the d-axis. Thus it enabled the controlling the stator reactive power through d-axis and the electromagnetic torque through q-axis, in accordance with (9) and (11). Concerning the grid-side converter, the grid voltage vector oriented control [3][8][12] was used, that enabled the control of the DC-link voltage, as well as the reactive power in this converter.

Table I shows the parameters of the simulated system. These parameters are used in all simulations.

**TABLE I**  
**Specifications of the simulated system.**

Specifications	
Machine parameters	Value
Apparent power	2.2 MW
Rated stator voltage	690 V
Rated angular frequency	376.99 rad/s
Mutual inductance	4.362 pu
Stator leakage inductance	0.102 pu
Rotor leakage inductance	0.110 pu
Stator resistance	0.0054 pu
Rotor resistance	0.0060 pu
Poles number	2
Inertia constant	0.5 s
Turbine parameters	Value
Rated power	2.0 MW
Inertia constant	4.0 s

### A. Case 1: Wind power generation composed by one DFIG

Fig. 4 shows a wind power generation system based on DFIG. The inductance ( $L_g$ ) filter limits the high-frequency ripple due to switching harmonics. The wind power system is connected to the power grid via a step-up transformer  $T$ .

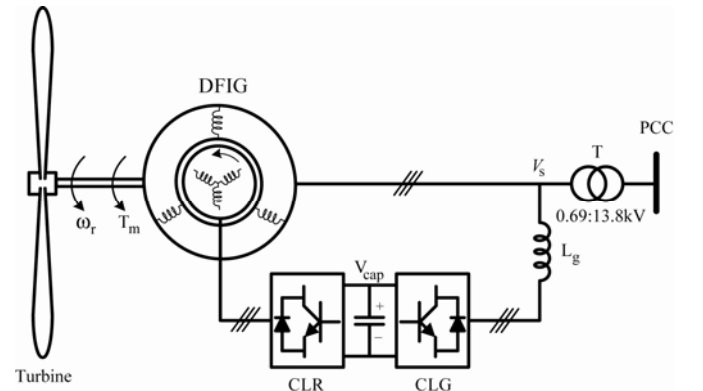


Fig. 4. Wind power generation based on DFIG.

In this simulation, a step change in the wind speed from 9.8 (sub-synchronous operation) to 13 m/s (super-synchronous operation) was applied at  $t = 20$  s.

The rotor speed reference value is derived of the  $C_p \times \lambda$ , characteristic curve of the turbine, where  $C_p$  is the power coefficient and  $\lambda$  is the tip speed ratio. Through the optimum value of the tip speed ratio, it is possible finds the rotor speed reference.

Fig. 5 shows the transient behavior of reference and actual rotor angular frequencies for MPPT.

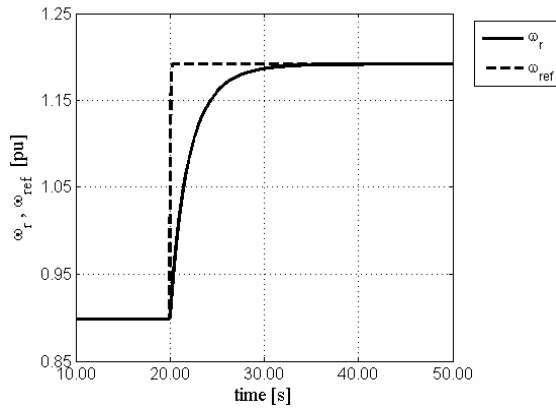


Fig. 5. Reference and actual rotor angular frequencies.

Figures 6 and 7 shows the stator and rotor currents in d-q axis.

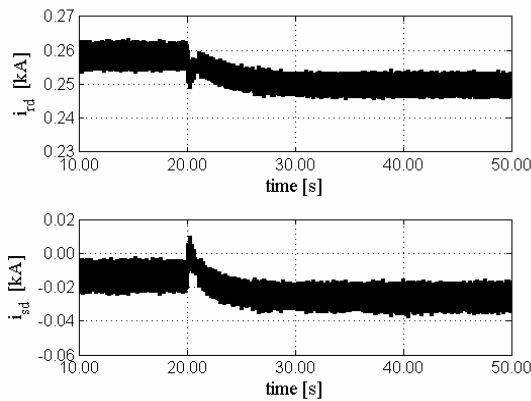


Fig. 6. Stator and rotor currents in d-axis.

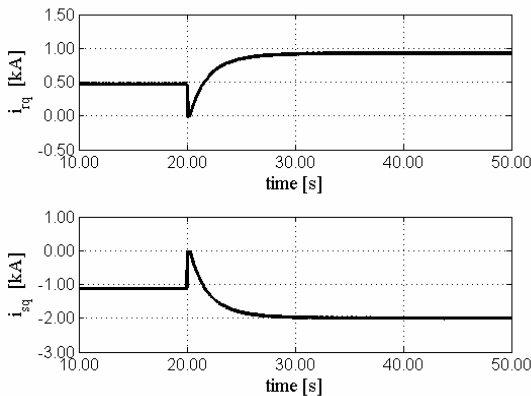


Fig. 7. Stator and rotor currents in q-axis.

Note that, in accordance with this result, the stator current is proportional to the rotor current in q-axis. In d-axis, there is no a proportional relationship between the stator and rotor currents, as can be seen in (17). However, these variables have low magnitudes, not implying in significant variations in the instantaneous currents in the stator phases.

Fig. 8 shows the behavior of current rotor for sub (upper) and super-synchronous (lower) operations.

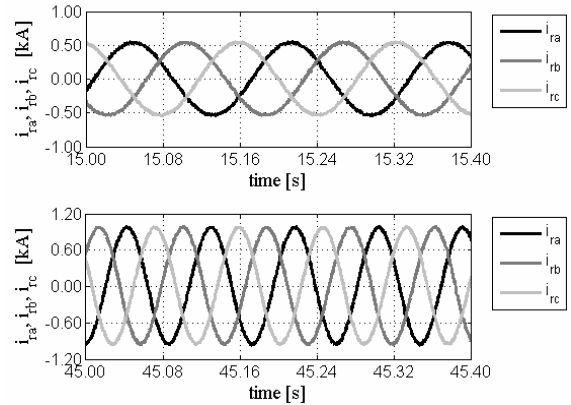


Fig. 8. Rotor currents in a,b,c coordinates.

Hysteresis band current modulation technique was used to synthesize rotor currents.

Fig. 9 shows the active and reactive stator power during wind speed dynamic variation.

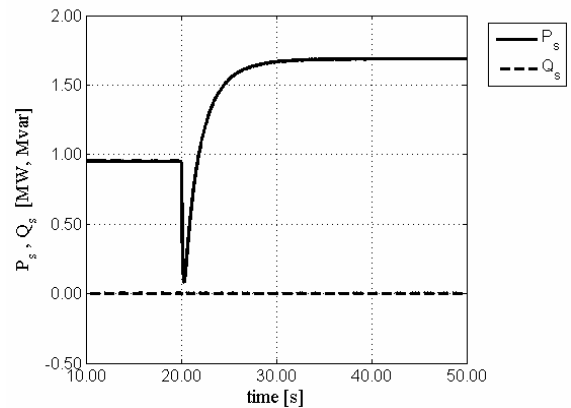


Fig. 9. Active and reactive stator power.

Fig. 9 shows that DFIG with MPPT using rotor speed control behaves as a non-minimum phase system, with respect to stator active power.

#### B. Case 2: Wind power generation composed by two paralleled DFIG

In this second case, the behavior of two paralleled DFIG system is evaluated. Thus, two identical systems to the system shown in Fig. 4 were paralleled, as shows the Fig. 10.

In Fig. 10, the inductances  $L_1$  and  $L_2$  indicate different distances, between each system and the step-up transformer  $T$ .

The system characteristics are as shown in Table I, as mentioned previously, for both machines.

The simulations were made, as described to follow: In both systems a step change in the wind speed was applied, thus the wind speed steps from 9.8 (sub-synchronous operation) to 13 m/s (super-synchronous operation) at  $t = 20$  s in system 1 and at  $t = 30$  s in system 2.

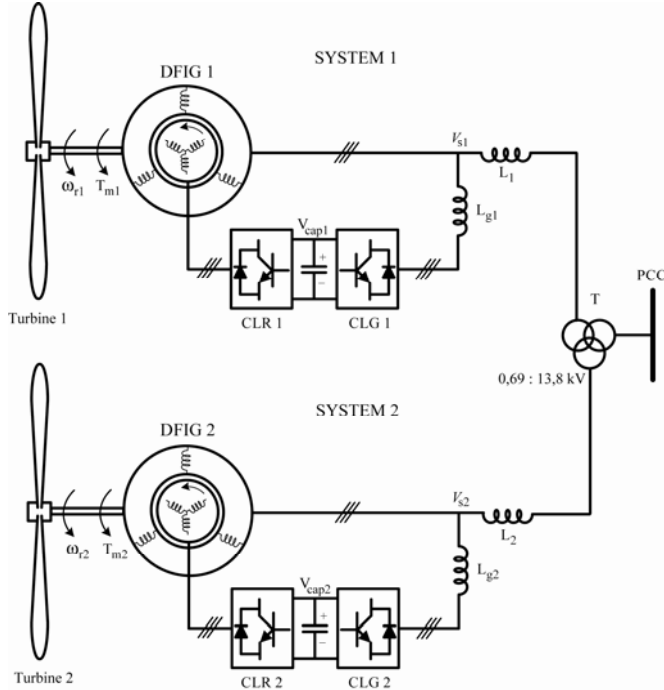


Fig. 10. Paralleled DFIG system.

Both DFIG systems used the same methodology to extraction of the rotor speed reference values shown in Fig. 4.

Fig. 11 shows the transient behavior of reference and actual rotor angular frequencies for the two systems.

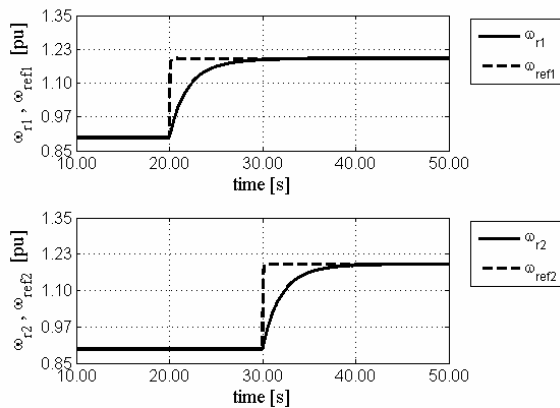


Fig. 11. Reference and rotor angular frequencies. System 1 (upper) and system 2 (lower).

Fig. 12 shows the active power generated by each wind turbine and the active power delivery to the network.

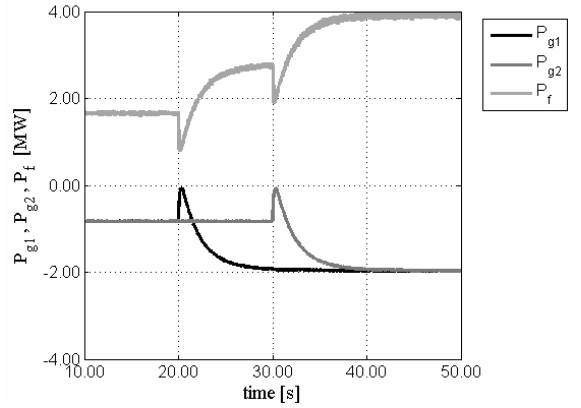


Fig. 12. Active power generated (system 1:  $P_{g1}$  and system 2:  $P_{g2}$ ) and active power delivery to the network ( $P_f$ ).

The simulations results proved that, if the power grid voltage is constant, DFIG has a current source behavior when connected to the grid and fed in its rotor by controlled current converter, in accordance with the mathematical equations of section III. Thus, for this condition, wind power turbines based on DFIG can be parallel-connected to the grid, increasing the power and reliability of electric energy generation.

### C. Case 3: Two paralleled DFIG system in ride-through operation

In this case, for the system shown in Fig. 10, occurs a short-circuit in PCC at  $t = 20$  s, during 500 ms. This fault leads voltage dip, to 20% of the rated voltage, in point of common connection (PCC). During simulation the wind speed remained constant.

Fig. 13 shows the stator flux in the system 1 (upper) and in the system 2 (lower), during voltage dip.

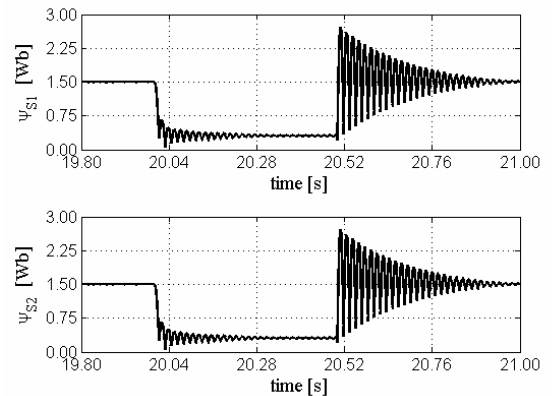


Fig. 13. Stator fluxes.

The stator flux oscillations shown in Fig. 13, occurs due the oscillations in the stator currents in dq-axis, as can be seen in (15) and (16).

Fig. 14 and Fig. 15 shows the instantaneous aggregate values ( $i_{\Sigma} = \sqrt{i_a^2 + i_b^2 + i_c^2}$ ) of stator and rotor currents, and

DC-link voltage for the system 2, respectively, during the fault.

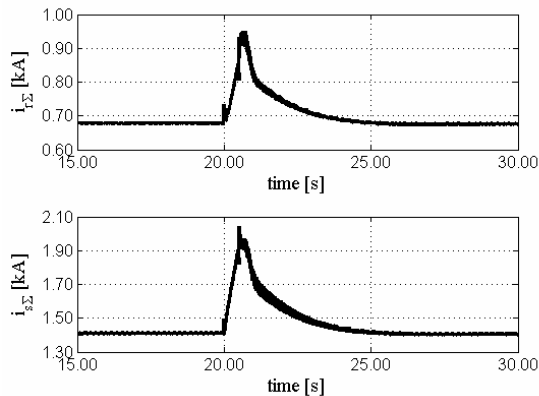


Fig. 14. Stator and rotor currents for the system 2.

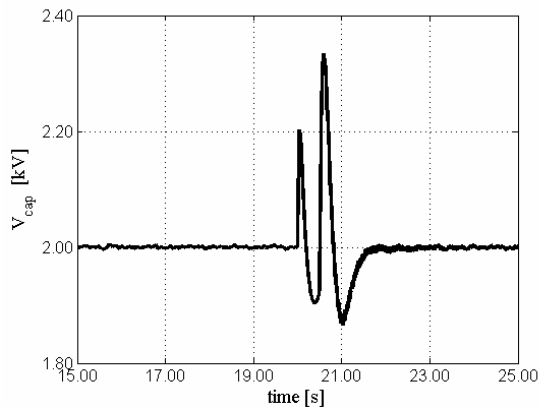


Fig. 15. DC-link voltage for the system 2.

Notice that, although has been applied a severe voltage dip, the magnitudes of the stator and rotor currents, for the simulated systems, reached moderated levels.

## V. CONCLUSION

The analysis has shown that DFIG, when current controlled through the rotor-side converter and connected to the grid, behaves as current source. This result suggests that the operating of wind systems equipped with DFIG and being parallel-connected, will work with no problem concerning to mutual interference system control, even under voltage-sag conditions at the point of common coupling (PCC).

In ride-through operation we can conclude, through simulation results shown, that DFIG lost the current source behavior. However, the magnitudes of the stator and rotor currents, for the simulated systems, reached moderated levels. Thus, auxiliary circuits were not inserted, in these systems, in order to limit overcurrents in the machine or overvoltage in the converters capacitors. The simulated model didn't use protection crowbar circuit, because the rotor and stator currents remained in admissible levels. The maximum CD-link voltage reached 1.25 p.u., while the maximum stator and rotor currents didn't exceed 1.45 p.u.

However, the ride-through operations for parallel connection of DFIG require a more detailed investigation. Thus, this subject will be again exploited in future studies.

## ACKNOWLEDGEMENT

The financial support provided by the Conselho Nacional de Desenvolvimento Científico e Tecnológico (CNPq), Coordenação de Aperfeiçoamento de Pessoal de Nível Superior (CAPES) and Fundação Carlos Chagas Filho de Amparo à Pesquisa do Estado do Rio de Janeiro (FAPERJ) is gratefully acknowledged.

## REFERENCES

- [1] ANEEL (Brasil). Banco de informações de geração. Disponível em: <<http://www.aneel.gov.br>>. Acesso em: 20 dez. 2006.
- [2] CRESESB (Brasil). Atlas do potencial eólico brasileiro. Disponível em: <<http://www.cresesb.cepel.br>>. Acesso em: 15 dez. 2006.
- [3] I. Boldea, "Variable speed generators". Boca Raton: CRC Press, 2006. 552 p. (The electric power engineering series).
- [4] J. G. Sloomweg, H. Polinder and W. L. Kling, "Dynamic modelling of a wind turbine with doubly fed induction generator". IEEE Power Engineering Society Summer Meeting, 2001. vol. 1, p. 644-649, 2001.
- [5] A. Petersson, "Analysis, modeling and control of doubly-fed induction generators for wind turbines". 2005. 165 f. PhD Thesis - Department of Energy and Environment, Chalmers University of Technology, Göteborg, 2005.
- [6] A. Petersson et al, "Modeling and experimental verification of grid interaction of a DFIG wind turbine". IEEE Transactions on Energy Conversion, vol. 20, N° 4, p. 878-886, 2005.
- [7] M. Yamamoto and O. Motoyoshi, "Active and reactive control for doubly-fed wound rotor induction generator". IEEE Transactions on Power Electronics, vol. 6, N° 4, p. 624-629, 1991.
- [8] R. Pena, J. C. Clare and G. M. Asher, "Doubly fed induction generator using back-to-back PWM converters and its application to variable-speed wind-energy generation". IEE Proceedings - Electric Power Applications, vol. 143, No 3, p. 231-241, 1996.
- [9] R. Pena, J. C. Clare and G. M. Asher, "A doubly fed induction generator using back-to-back PWM converters supplying an isolated load from a variable speed wind turbine". IEE Proceedings - Electric Power Applications, vol. 143, No 5, p. 380-387, 1996.
- [10] W. Leonhard, "Control of electrical drives". 3a. ed. New York: Springer, 2001. 470 p.
- [11] R. W. De Doncker and D. W. Novotny, "The universal field oriented controller". IEEE Transactions on Industry Applications, vol. 30, No 1, p. 92-100, 1994.
- [12] K. F. Silva, "Controle e integração de centrais eólicas na rede elétrica com geradores de indução duplamente alimentados". 2006. 240 f. Tese (Doutorado) - Departamento de Engenharia de Energia e Automação Elétricas, USP, São Paulo, 2006.